THE ASTROPHYSICAL JOURNAL, 281: 276–285, 1984 June 1

TEMPERATURES AND SURFACE GRAVITIES OF DB WHITE DWARFS

J. B. OKE
Palomar Observatory, California Institute of Technology

AND

V. WEIDEMANN AND D. KOESTER
Institut für Theoretische Physik und Sternwarte, University of Kiel
Received 1983 July 11; accepted 1983 December 1

ABSTRACT

Multichannel observations or reobservations of all DB white dwarfs accessible from Palomar Observatory, reduced and calibrated with the AB_{79} program of Oke and Gunn, have been compared by least squares fitting procedures with energy distributions calculated from new model atmospheres with He:H = 10^5 and reduced metal content He:C = 10^6. The surface gravities and temperatures derived reveal for the first time a definitive cooling sequence for the DB stars, with a narrow mass distribution comparable to that of the DA white dwarfs. The mass range, $0.55 \pm 0.10\ M_\odot$, almost coincides with the range derived for DA, DC, and C_2 stars and therefore suggests that the progenitors for all these stars are the same.

Spectroscopic distance determinations and comparison with cooling ages demonstrate that DB stars account for about one-tenth of the total white dwarf birthrate. Attempts to calibrate calculated Strömgren colors with multichannel scans reveal that the observational scatter of Strömgren photometry is too large to allow reliable g and $T_{\rm eff}$ determinations for individual DB stars.

Subject headings: spectrophotometry — stars: atmospheres — stars: white dwarfs

I. INTRODUCTION

After more than a decade of work on degenerate stars with helium-rich atmospheres, the origin and nature of the DB white dwarfs are still unexplained. In his review article Liebert (1980) gives some reasons why the atmospheric and stellar parameters for helium-atmosphere degenerates are not nearly as well determined as those for the "normal" DA white dwarfs with hydrogen-rich atmospheres. These mainly concern the larger difficulties and uncertainties in the theoretical treatment of the model atmospheres, some of which were in the process of being overcome when Liebert's review was written.

DB stars are much less numerous than DA stars in space and thus are on the average considerably fainter, which makes high-quality observations more difficult. With the closest DB at a distance of about 40 pc, visual magnitudes are generally beyond 14 mag. In contrast to the DA stars, there are only very few DBs with even uncertain trigonometric parallaxes or distances determined from companions or cluster membership (see Koester, Schulz, and Wegner 1981).

Spectra are in general of low resolution, which, when combined with the fact that the theoretical sensitivity of line profiles on atmospheric parameters—especially surface gravity—is much smaller than in the DA case, explains why their analysis has up to now not produced reliable results. Thus the important question remained open as to whether the DB masses differ systematically from those of the DA stars, i.e., if DB and DA stars have fundamentally different progenitors (see Weidemann 1975). Johnson colors are completely useless—all DBs cluster at about (−0.95), (−0.10) in the $(U-B)$-$(B-V)$ diagram—and Strömgren photometry is likewise so insensitive to $T_{\rm eff}$ and g that in view of the observational and calibration uncertainties, neither individual nor mean atmospheric parameters can be determined with confidence (see Koester, Schulz, and Wegner 1981).

Multichannel spectrophotometry (MCSP) developed and carried out at the Palomar 5 m telescope by Oke (1974) and Greenstein (1976) provided new data, but a first analysis as presented by Greenstein (1976) based on monochromatic MCSP color indices and Shipman model fluxes (Shipman 1979) proved disappointing, with large scatter in the $(U-B)$-$(G-R)$ diagram, and no possibility of model fits. He has recently added new MCSP data and rediscussed the fits to the models (Greenstein 1984).

A serious handicap consisted of the fact that for some DB stars information was rather incomplete, with only MCSP data, Strömgren photometry, or spectra available. Thus calibration of Strömgren photometry with the help of MCSP data—in the way it was done by Schulz (1978) for the DA stars—was impossible. Because of this situation, one of us (J. B. O.) agreed to observe or reobserve all northern DB stars with the Palomar telescope. After the program was carried out in 1979 and 1980, the new MCSP data were first evaluated according to the Schulz (1977) method (which uses broad-band colors instead of monochromatic color indices and which has been shown to be superior in the DA case; Koester, Schulz, and Weidemann 1979), by one of us (V. W.). Comparison with Koester model predictions revealed for the first time a clear, narrow-g temperature sequence, if only for the data from five of the seven observing nights. We thus decided to evaluate the MCSP data at Kiel with computerized complete least squares fits. The results are presented in this paper. Temperatures and gravities are now so well determined that spectroscopic distances, birthrates, average masses, and a mass distribution can be calculated. In § II we give the observations, § III describes the model atmospheres and procedures of evaluation, § IV gives the results, including the derived properties of the DB stars, § V deals with the Strömgren photometry and calibration, and in § VI we discuss and summarize the results.

II. OBSERVATIONS

The observations were carried out with the multichannel spectrophotometer at the Palomar 5 m telescope (see Oke 1974) with a resolution of 80 Å/160 Å. The list comprised all DB stars accessible from the location; 35 stars were observed on seven nights (191, 192, 193, 194, 196, 197, 198; corresponding to 1979 October 25, 27, 28, and 29, 1980 January 26, February 25, and July 16, respectively). The scans were calibrated by reference to standard sdG stars (BD +17°4708, HD 19445, HD 84937, and BD +26°2606) on the absolute scale AB_{79} (Oke and Gunn 1983), which differs from Hayes and Latham (1975) by small amounts of the order of $\Delta(U-B) = -0.01$, $\Delta(G-R) = +0.03$, depending on the standards which were used on an individual night. The quality of the individual measurements varies; low-quality scans are sometimes caused by malfunctions in individual channels, sometimes by bad observing conditions. The least squares analysis (below) reveals this as well as direct inspection. Examples of scans are given in Figure 1.

The scan of G242-63, which turned out to be a DC (with $T_{\rm eff} < 10{,}000$ K) rather than a DB star, gives some impression of the remaining uncertainties. Where systematic effects were detected, the channels were omitted in the least squares fit procedure (see below). Besides G242-63 (WD 0038+73), three further stars did not belong to the DB category: LB 378A (0855+60), a cooler object, probably C_2, as revealed by SIT spectra; GD 323 (1302+59), a hot DAB, with hydrogen lines (see also Liebert and Wesemael 1983); and G227-5 (1728+56), a peculiarly hot-looking star (18,000 K) without He I but numerous C I lines.

One other object, the peculiar DB emission binary G61-29 (1303+18), was also excluded from further analysis. The remaining 30 DB stars are listed in Table 1, which contains the pertinent parameters, along with WD coordinate [McCook-Sion Catalog 1977], designation, Greenstein number, visual magnitude, and night of observation.

III. MODEL ATMOSPHERES AND METHOD OF EVALUATION

The calculation of model atmospheres followed the procedures described elsewhere (Koester 1980), with slight modifications and extensions. Numerical methods were improved, which resulted especially in a better definition of the temperature stratification in the outermost layers. However, this influences only the cores of the strongest lines.

The He/H ratio was kept at 10^5, since at 10^4, the value preferred by Wickramasinghe (1979, 1983) and Wickramasinghe and Reid (1983), the Lyα line would appear too strong to be compatible with *IUE* observations.

The metal abundances were changed in view of the results of the analysis of the cooler helium-rich atmosphere DC and C_2 stars (Koester, Weidemann, and Zeidler-K. T. 1982) to C/He = 10^{-6} instead of metals/He = 1.5×10^{-5}. Even this is probably too high a carbon abundance since *IUE* spectra do not show C I or C II lines (Wickramasinghe 1983). However, we checked and found that a further reduction of the carbon abundance does not change the energy distribution in the visible,

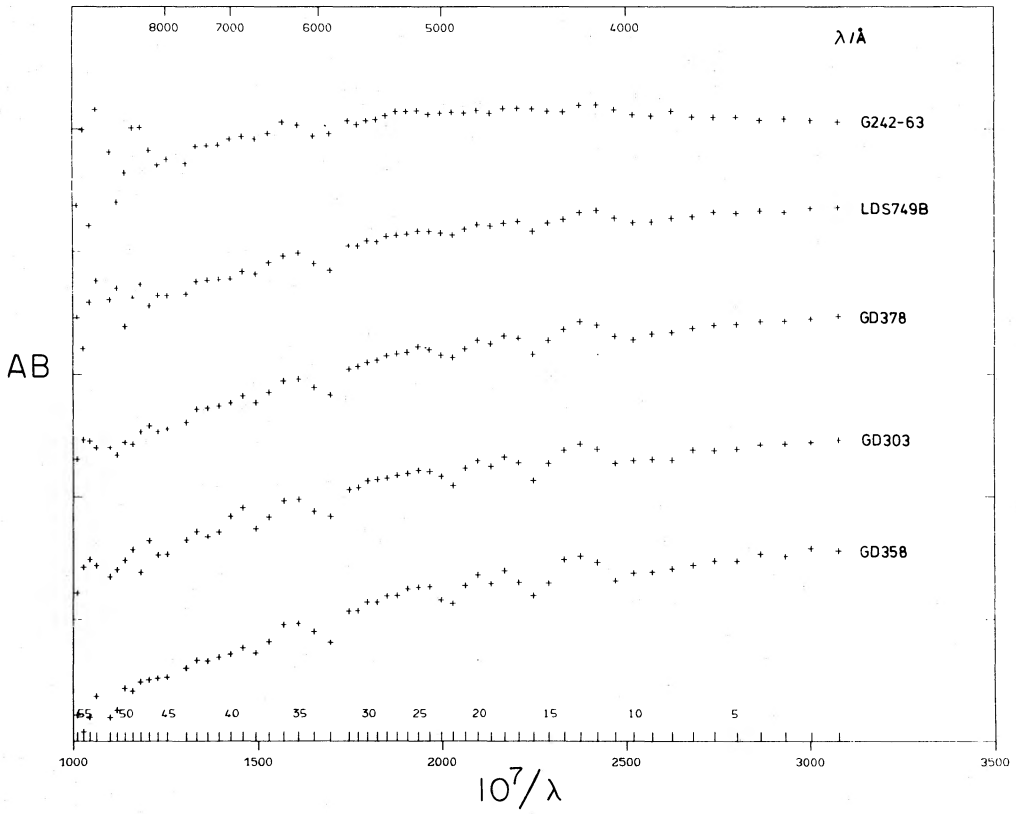

FIG. 1.—Examples of multichannel observations: G242-63 (DC, $T_{\rm eff}$ = 9600 K, night 191), LDS 749B (DB, 13,000 K, night 192), GD 378 (DB, 16,000 K, night 193), GD 303 (DB, 17,000 K, night 196), GD 358 (25,000 K, night 198). The ticks on the vertical scale are 1 mag apart. On the lower scale, individual measuring points (two belonging to each channel) are marked for the discussion in § III.

TABLE 1

ATMOSPHERIC PARAMETERS AND DERIVED PROPERTIES FOR DB STARS

No.	WD Designation	Name	EG or Gr Number	V	Night	T_{eff}	log g	M(g)	log $R/R_{\odot}$(g)	χ^2	Set No.	d(pc)	Notes
1	0000-17	G266-32	508	15.2	193	12110(170)	[7.52(0.67)	0.32(0.28)	-1.79(0.15)	1.0	III	46.9(16.3)]	
2	0002+72	GD 408	305	14.3	191	13310(190)	7.69(0.36)	0.40(0.18)	-1.83(0.09)	0.6	II	40.3(8.1)	
3	0017+13	Feige 4	3	15.3	191	17540(400)	8.01(0.12)	0.57(0.07)	-1.91(0.03)	1.2	II	71.5(5.3)	
4	0100-06	G270-124	513	13.8	192	19000-23000	...	...	...	...	...	...	a
5	0112+10	PG179-39	409	15.4	192	28900(560)	8.07(0.15)	0.61(0.10)	-1.92(0.04)	1.3	II	94.3(9.3)	
6	0119-00	G271-47	516	16.0	192	[24000]	...	...	...	>8	...	...	b
7	0300-01	GD 40	384	15.5	191	13730(200)	7.85(0.32)	0.48(0.18)	-1.86(0.08)	1.3	II	67.3(12.5)	c
8	0435+41	GD 61	315	14.9	192	16410(370)	8.05(0.14)	0.60(0.09)	-1.92(0.04)	1.0	II	51.6(4.7)	
9	0437+13	LP475-242	316	14.8	191	15090(260)	7.91(0.19)	0.51(0.11)	-1.88(0.05)	1.3	II	55.1(6.3)	e
10	0716+40	GD 85	216	14.9	193	16280(310)	[7.86(0.14)	0.48(0.08)	-1.87(0.03)	2.7	II	58.3(4.8)]	
11	0841+26	Ton 10	291	14.5	194	17310(380)	8.24(0.12)	0.72(0.08)	-1.97(0.04)	1.1	II	48.0(4.0)	
12	0845-18	LDS 235B	63	15.6	194	[17800]	...	...	...	>7	...	...	b
13	1011+57	GD 303	386	14.6	196	17180(400)	7.79(0.12)	0.45(0.06)	-1.85(0.03)	1.0	II	58.6(4.1)	
14	1046-01	GD 124	387	15.8	196	13730(200)	8.00(0.34)	0.57(0.21)	-1.90(0.09)	2.3	III	70.7(14.7)	
15	1048+04	LP551-21	...	16.7	196	12850(170)	[7.48(0.46)	0.30(0.18)	-1.78(0.10)	3.2	II	136.1(13.6)]	
16	1107+26	Ton 573	77	15.9	197	14390(250)	8.12(0.30)	0.64(0.19)	-1.94(0.08)	0.9	III	70.1(13.4)	
17	1241+65	GD 479	292	16.8	197	13340(210)	8.17(0.51)	0.68(0.34)	-1.95(0.15)	1.8	III	93.8(31.5)	
18	1304+15	GD 268	390	17.0	197	[13200]	...	...	...	3.5	III	...	
19	1403-01	G64-43	272	15.9	197	14440(260)	...	...	...	...	...	...	
20	1459+82	G256-18	393	14.8	197	15030(270)	[7.52(0.21)	0.32(0.09)	-1.79(0.005)	0.8	III	63.8(7.0)]	
21	1542+18	GD 190	193	14.6	197	22670(990)	[8.22(0.15)	0.71(0.10)	-1.97(0.04)	1.0	III	53.7(5.7)]	
22	1612-11	GD 198	194	15.5	198	19270(630)	8.02(0.10)	0.58(0.06)	-1.91(0.03)	1.5	II	80.6(5.4)	
23	1645+32	GD 358	239	14.0	198	24610(480)	7.84(0.16)	0.47(0.05)	-1.86(0.04)	1.4	II	43.6(4.2)	d
24	1709+23	GD 205	224	15.0	198	22750(900)	8.03(0.14)	0.58(0.09)	-1.91(0.04)	1.1	II	65.5(5.7)	
25	1822+41	GD 378	242	14.0	193	15590(270)	7.93(0.17)	0.53(0.10)	-1.89(0.04)	0.9	II	41.0(4.2)	
26	1940+37	L1573-31	133	14.5	193	15820(270)	7.71(0.16)	0.41(0.08)	-1.83(0.04)	1.0	II	53.3(4.8)	
27	2129+00	LDS 749B	145	14.7	192	13150(190)	7.86(0.40)	0.48(0.22)	-1.87(0.10)	0.7	II	42.6(9.8)	f
28	2130-04	GD 233	146	14.5	192	17500(390)	8.14(0.11)	0.66(0.08)	-1.94(0.03)	1.4	II	44.3(3.4)	
29	2144-07	L930-80	149	14.8	193	15540(260)	8.14(0.18)	0.66(0.12)	-1.94(0.05)	1.0	II	45.6(5.4)	
30	2251+74	GD 554	504	16.7	192	15720(270)	7.69(0.16)	0.40(0.08)	-1.83(0.04)	1.4	II	129.8(12.0)	

[a] No convergence of minimum finding procedure.
[b] Low-quality scan.
[c] DB with metal lines; see Shipman and Greenstein 1983.
[d] Pulsating DB; see discussion in § VI.
[e] Hyades, $d = 44$ pc; see Koester, Schulz, and Wegner 1981.
[f] Trigonometric parallax, $d = 43$ pc.

and thus the analysis is carried out with the C/He ratio given above.

The model grid has been extended to cover the range $12{,}000 \leq T_{\rm eff} \leq 40{,}000$ K and log g from 7.0 to 8.5. For the calculation of synthetic spectra, some additional He I lines below 4000 Å have been taken into account, which were not included previously. The approximation to the Stark broadening theory (Griem 1974) has been improved, leading to changes in the line profiles especially of λ4026 and λ4388. The profile of the blend λ4388 + λ4472 is now in much better agreement with observations. *UBV* and Strömgren colors as well as monochromatic Greenstein indices and absolute visual magnitudes are presented in Table 2.

The Schulz broad-band colors R_{13} and R_{48}, replacing the Greenstein indices $(U-B)$ and $(G-R)$, are defined by average flux ratios in the wavelength intervals 1, 3, 4, 8: $\lambda\lambda$3300–3700, 4200–4600, 4600–5200, and 6800–7200 Å, respectively; i.e., $R_{ik} = -2.5(\log \langle F\rangle_i - \log \langle F\rangle_k)$. Compare Koester, Schulz, and Weidemann (1979), where the definition should be corrected to

$$m_i = -2.5 \log \left[\int_{\lambda_i}^{\lambda_{i+1}} F_\lambda \, d\lambda / (\lambda_{i+1} - \lambda_i) \right].$$

Calculated and observed values are plotted in the R_{13}-R_{48} diagram of Figure 2.

Although the wavelength intervals were originally chosen to provide a g-sensitive index for the DA stars, they turned out to

TABLE 2

JOHNSON AND STRÖMGREN COLORS AND GREENSTEIN MULTICHANNEL INDICES

	JOHNSON			STRÖMGREN		MC			
$(T_{\rm eff}/1000)/\log g$	$B-V$	$U-B$	M_v	$b-y$	$u-b$	$U-B$	$G'-R'$	$G-R$	$U-V$
12/7.0	0.010	−0.888	10.86	0.057	0.083	0.015	−0.402	−0.343	−0.131
14/7.0	−0.034	−0.924	10.48	0.012	0.031	0.028	−0.509	−0.436	−0.194
16/7.0	−0.049	−0.922	10.19	−0.002	0.044	0.098	−0.594	−0.505	−0.177
18/7.0	−0.050	−0.906	9.96	−0.008	0.073	0.161	−0.642	−0.538	−0.139
20/7.0	−0.057	−0.913	9.84	−0.014	0.062	0.153	−0.657	−0.552	−0.158
22/7.0	−0.073	−0.931	9.73	−0.024	0.034	0.135	−0.677	−0.571	−0.191
24/7.0	−0.093	−0.953	9.60	−0.040	0.001	0.110	−0.706	−0.600	−0.241
26/7.0	−0.113	−0.975	9.49	−0.054	−0.035	0.087	−0.729	−0.623	−0.286
28/7.0	−0.134	−1.001	9.39	−0.067	−0.075	0.050	−0.746	−0.643	−0.339
30/7.0	−0.152	−1.025	9.28	−0.078	−0.113	0.019	−0.760	−0.660	−0.383
35/7.0	−0.188	−1.080	9.03	−0.098	−0.202	−0.068	−0.790	−0.693	−0.494
40/7.0	−0.216	−1.214	8.79	−0.114	−0.270	−0.131	−0.818	−0.723	−0.579
12/7.5	0.009	−0.891	11.33	0.058	0.077	0.006	−0.400	−0.342	−0.139
14/7.5	−0.034	−0.935	10.96	0.023	0.013	0.002	−0.501	−0.427	−0.213
16/7.5	−0.050	−0.949	10.67	0.003	−0.001	0.041	−0.580	−0.492	−0.223
18/7.5	−0.049	−0.937	10.44	−0.001	0.023	0.113	−0.633	−0.528	−0.177
20/7.5	−0.052	−0.946	10.29	−0.002	0.013	0.111	−0.653	−0.543	−0.189
22/7.5	−0.063	−0.956	10.20	−0.010	−0.004	0.095	−0.661	−0.553	−0.214
24/7.5	−0.080	−0.976	10.08	−0.022	−0.034	0.071	−0.684	−0.575	−0.255
26/7.5	−0.099	−0.993	9.97	−0.037	−0.061	0.054	−0.711	−0.602	−0.295
28/7.5	−0.118	−1.011	9.86	−0.052	−0.090	0.034	−0.735	−0.626	−0.337
30/7.5	−0.137	−1.032	9.76	−0.064	−0.123	0.009	−0.752	−0.645	−0.378
35/7.5	−0.177	−1.084	9.51	−0.088	−0.206	−0.069	−0.784	−0.683	−0.485
40/7.5	−0.206	−1.127	9.28	−0.106	−0.273	−0.134	−0.812	−0.714	−0.573
12/8.0	0.007	−0.895	11.94	0.056	0.071	−0.004	−0.400	−0.343	−0.149
14/8.0	−0.036	−0.946	11.56	0.023	−0.003	−0.023	−0.492	−0.423	−0.233
16/8.0	−0.054	−0.968	11.27	0.007	−0.033	0.002	−0.571	−0.481	−0.254
18/8.0	−0.053	−0.972	11.05	0.006	−0.031	0.048	−0.618	−0.515	−0.232
20/8.0	−0.053	−0.976	10.88	0.007	−0.034	0.068	−0.649	−0.536	−0.226
22/8.0	−0.059	−0.989	10.79	0.003	−0.052	0.051	−0.654	−0.542	−0.247
24/8.0	−0.072	−0.998	10.69	−0.006	−0.070	0.035	−0.669	−0.557	−0.275
26/8.0	−0.089	−1.019	10.58	−0.019	−0.100	0.011	−0.690	−0.579	−0.317
28/8.0	−0.107	−1.033	10.47	−0.033	−0.123	−0.005	−0.714	−0.603	−0.353
30/8.0	−0.124	−1.048	10.37	−0.047	−0.146	−0.021	−0.735	−0.626	−0.387
35/8.0	−0.165	−1.092	10.13	−0.074	−0.217	−0.082	−0.773	−0.668	−0.483
40/8.0	−0.197	−1.134	9.89	−0.095	−0.282	−0.145	−0.803	−0.702	−0.572
12/8.5	0.004	−0.898	12.68	0.055	0.066	−0.012	−0.405	−0.346	−0.157
14/8.5	−0.039	−0.954	12.31	0.023	−0.016	−0.042	−0.492	−0.422	−0.250
16/8.5	−0.060	−0.986	12.02	0.008	−0.060	−0.033	−0.562	−0.477	−0.287
18/8.5	−0.060	−0.999	11.79	0.009	−0.074	−0.007	−0.607	−0.506	−0.281
20/8.5	−0.058	−1.006	11.61	0.014	−0.083	0.016	−0.637	−0.526	−0.271
22/8.5	−0.062	−1.019	11.50	0.014	−0.099	0.010	−0.653	−0.538	−0.284
24/8.5	−0.071	−1.028	11.42	0.007	−0.114	−0.007	−0.657	−0.545	−0.306
26/8.5	−0.085	−1.040	11.32	−0.003	−0.133	−0.023	−0.675	−0.563	−0.336
28/8.5	−0.100	−1.058	11.22	−0.016	−0.159	−0.045	−0.695	−0.583	−0.374
30/8.5	−0.116	−1.071	11.12	−0.029	−0.180	−0.060	−0.716	−0.605	−0.407
35/8.5	−0.155	−1.106	10.89	−0.059	−0.236	−0.106	−0.758	−0.651	−0.490
40/8.5	−0.189	−1.144	10.66	−0.082	−0.295	−0.160	−0.791	−0.687	−0.573

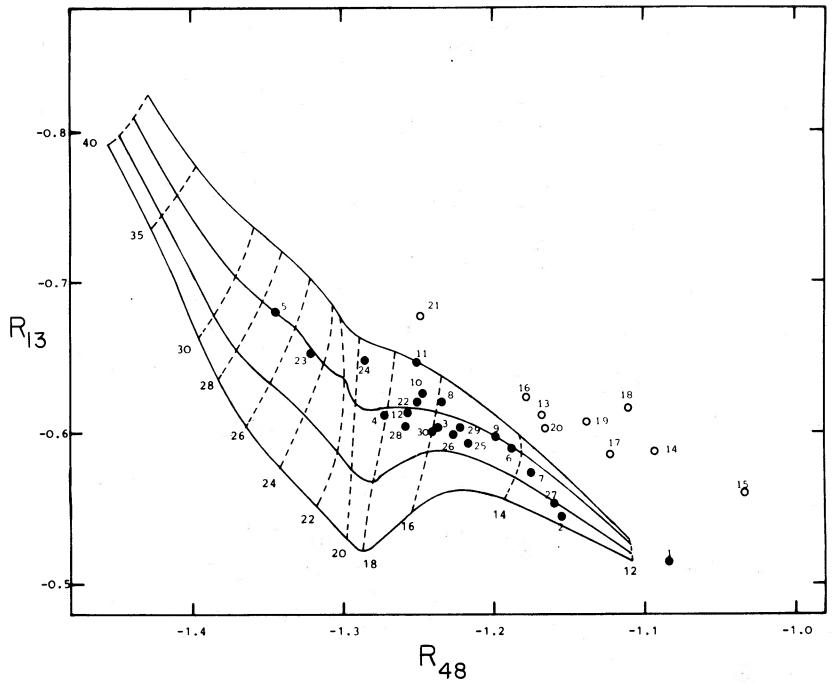

FIG. 2.—R_{13}-R_{48} diagram [broad-band MC $(U-B)/(G-R)$ colors, see text] of DB stars. Closed circles are observations from nights 191, 192, 193, 194, 198, while open circles are for nights 196, 197. Plotted on AB_{79} calibrations (Oke and Gunn 1983). Stars are identified with running numbers from Table 1. Solid lines are constant log g from theoretical models (8.5, 8.0, 7.5, 7.0 from top). Broken lines are constant $T_{\rm eff}$(40,000–12,000 K), identified by numbers in a larger type size.

be also usable in the DB case. The choice avoids the ranges which are more uncertain because of calibration ($\lambda\lambda$3700–4200) or multichannel resolution changes. The advantage of using broad-band colors lies in the fact that the averages taken tend to smooth out statistical scatter of individual scanner points. This has been demonstrated in the DA case by Koester, Schulz, and Weidemann (1979) and is also evident here by the large reduction of scatter in Figure 2 compared with the $(U-B)$-$(G-R)$ diagrams of Greenstein (1976) and Koester (1979). However, it is also evident from Figure 2 that the observing conditions play a major role: whereas the location of the stars observed on nights 191–194, which were completely clear, form a sequence which follows roughly the theoretical expectation, the points obtained for stars observed during nights 196 and 197, which were subject to fog and thin cloud conditions, differ systematically in colors by 0.05–0.10 mag and should be given very low weight. This happens because the wavelength dependence of the extinction law changes under these conditions and varies with the amount of cloud cover.

In fitting the multichannel observations to the model atmospheres, one must allow for the fact that some points are not determined as accurately as others either because of absolute calibration uncertainties and sharp atmospheric extinction features, or because some channels in the instrument are consistently not as stable as others. Defining set I to consist of all 44 points shortward of 7740 Å corresponding to channels 2–23, set II is derived as follows. Points 9–13 are deleted because they deviate systematically from the models because of absolute calibration uncertainties in the neighborhood of the H and K lines of Ca II. Points 38, 43, and 44 are influenced by the atmospheric A and B bands and are dropped. Points 33–36 and 39–40 are deleted because they correspond to three channels which are somewhat unstable. Set III omits, in addition, channel 13 (points 23 and 24) and channel 5 (points 7 and 8), which are known to misbehave occasionally. The final least squares fits are based on sets II and III.

The least squares fitting method used is exactly the same as described in Koester, Schulz, and Weidemann (1979). The observations are the N individual scan points (with N ranging from 25 to 29 for the two sets discussed above) which are compared with theoretical "scans" constructed from the synthetic spectra using wavelength points and channel widths identical to those of the observations.

The final solution of $T_{\rm eff}$ and log g is defined by the minimum of χ^2, with

$$\chi^2 = \sum_{i=1}^{i=N} \frac{(\epsilon_i/\sigma_i)^2}{N-2}, \qquad (1)$$

where ϵ_i are the individual residuals between observed scan and theory, and σ_i are the standard deviations of the observations, assumed to be 0.02 mag for all channels.

In order to justify the procedure, a few examples are given in Table 3, in which the stars are ordered according to quality as judged by inspection of the observed scatter.

For the results in Table 1, in each case the solution corresponding to the lowest χ^2 was taken and indicated by the set number. In cases where the results in $T_{\rm eff}$ and log g did not change in going from set II to III, set III was disregarded. Set III is adopted primarily for the data of nights 196 and 197.

Uncertainties for the chosen effective temperatures and surface gravities are derived as in Koester, Schulz, and Weidemann (1979).

IV. RESULTS

The numerical results of the procedure outlined in § III are given in Table 1 and displayed in Figure 3.

Table 1 lists in order: WD number, McCook and Sion (1977)

TABLE 3

LEAST SQUARES FIT SOLUTION FOR DB SCANS

STAR	V	NIGHT	χ^2 OF FINAL SOLUTION Set I	Set II	Set III	SCATTER
L1573-31	14.5	193	3.18	1.02	1.00	small
LDS 749B	14.7	192	2.90	0.73	0.68	small
GD 358	14.0	198	2.81	1.42	1.58	small
GD 554	16.7	192	3.72	1.42	1.47	small
GD 303	14.6	196	4.42	0.96	0.83	small
GD 124	15.8	196	5.76	2.47	2.29	large
GD 190	14.6	197	265[a]	391[a]	0.97	ch. 13 off
Ton 573	15.9	197	3.97	2.49	0.88	ch. 5 off
G256-18	14.8	197	240[a]	354[a]	0.84	ch. 5 + 13 off
Number of points			44	29	25	

[a] These large values occur because the formal solution includes very large errors in channel 13. These disappear when channel 13 is removed in set III.

designation, name, EG or Greenstein number, visual magnitude, observing-night number, effective temperature $T_{\rm eff}$, surface gravity log g, mass and radius (derived with the mass-radius relation of Hamada and Salpeter 1961 for C interior composition), with uncertainties in parentheses, χ^2, set number (see § III), and distance.

Results in brackets are unreliable, either because of no clear solution for the minimum finding procedure or because of sets of poor quality. Figure 3 plots the results (the stars are identified by the numbers in the first column of Table 1). Figure 4 shows the corresponding mass distribution. The mass range is $0.525 \pm 0.12\ M_\odot$ for all (25) stars, or $0.55 \pm 0.10\ M_\odot$ if the uncertain objects (in brackets) are omitted.

With the spectroscopic distances of Table 1, we obtain the space distribution shown in Table 4. This diagram (Weidemann 1967; Sion and Liebert 1977) demonstrates completeness out to $m_v \approx 15$ mag. It remains essentially unchanged if instead of individual values of log g, a constant value of 8 is assumed for the spectroscopic distance determination. The corresponding space density is 1.5×10^{-5} DB white dwarfs per pc^3 out to $m - M = 3.5$ (or 50 pc) or 10^{-5} DBs per pc^3 (out to $m - M = 4.5$, or 80 pc).

The closest DB star, GD 408, is at $d = 40$ pc. The space densities must be corrected for (*a*) incompleteness in the ensemble, and (*b*) neglect of DBs south of $\delta = -20°$. Twelve out of a total of 21 cataloged DBs with $\delta > -20°$ and $m_v < 15$ mag are included in our final ensemble. Therefore, the correction factor for incompleteness should be ~ 2. The southern sky fraction amounts to 33% of the sphere, corresponding to a further correction factor of DBs of 1.5, so that the total space densities of DBs should be 4.5×10^{-5} DBs per pc^3. This corresponds, with a cooling age of 2×10^8 yr down to 12,000 K (Koester 1972), to a DB birthrate of 2.2×10^{-13} DBs per pc^3 yr^{-1}, which is about one-tenth of the total white dwarf birthrate (2×10^{-12} WDs per pc^3 yr^{-1}, Weidemann 1977). This has to be compared with earlier estimates of the DB fraction by Greenstein (1969), who found in his sample of blue GD stars 17% DBs, and by Weidemann (1979), who rediscussed the material and estimated the DB fraction to be between 10% and 15%. For the cooler helium-rich DC and C_2 stars Weidemann derived—with larger uncertainties—a birthrate amounting to 12% of the total, thus not contradicting the simplest assumption that all DC and C_2 stars are cooled-down DBs. Comparisons of observed luminosity distributions, on the other hand, by Sion and Liebert (1977) and Sion (1979) (see also Greenstein 1984) show that helium-rich degenerates become relatively more numerous for fainter absolute magnitudes. This has been taken as observational support for the hypothesis that a changeover occurs from DA to non-DA atmospheres, caused by convective mixing of thin hydrogen surface layers (Koester 1976; Vauclair and Reisse 1977). For a more comprehensive discussion see Liebert (1980). The smaller DB birthrate derived above thus strengthens this hypothesis but clearly more work is necessary in order to settle the question. Difficulties arise not

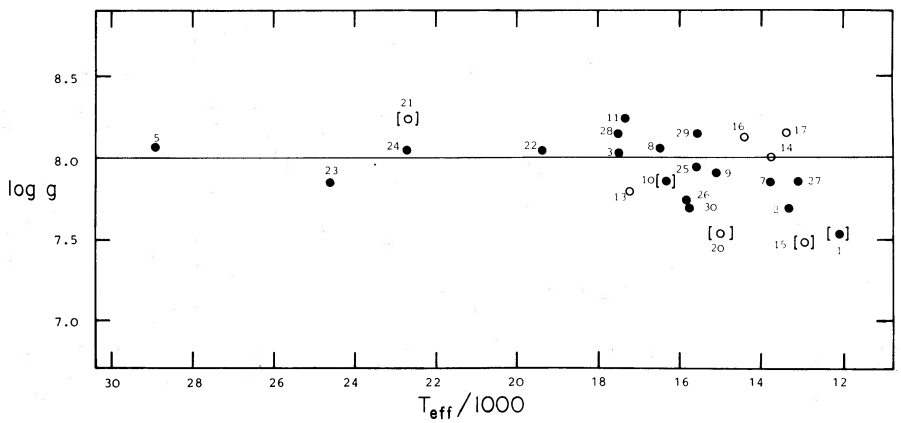

FIG. 3.—Effective temperature and surface gravity of DB stars (cf. Table 1). Closed circles are nights 191, 192, 193, 194, and 198, while open circles are nights 196 and 197. Brackets indicate uncertain results.

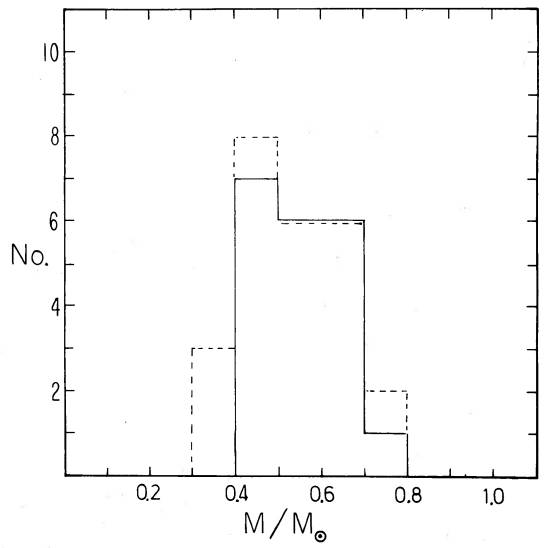

FIG. 4.—Relative mass distribution, $M(g)$, for DB stars. The broken lines are for the total ensemble of 25 stars. The solid lines are for the ensemble of 20 stars with reliable results.

only from the general scarcity of the statistical material at fainter magnitudes but also from the fact that it is not yet possible to distinguish between hydrogen- and helium-dominated atmospheres for the coolest degenerates.

V. STRÖMGREN PHOTOMETRY

Integrating over the sensitivity function of the Strömgren filters and using the transformation constants of Schulz (1978), "Strömgren colors" have been computed from the scans and compared with the observed colors (see Koester, Schulz, and Wegner 1981; Wegner 1983). If the transformation is correct, the resulting points should scatter around a line with a 45° slope going through the origin. For $b - y$ (Fig. 5, *left*) such a correlation is not visible; for $u - b$ (Fig. 5, *right*) a correlation with shifted zero point seems to be present.

TABLE 4

SPACE DISTRIBUTION OF DB WHITE DWARFS

	$m - M$				
M_v	2	3	4	5	6
10.5.....	0	1	4	2	1
11.5.....	0	7	8	1	1

If the slopes of the transformations are fixed at unity, a formal computation of the zero points gives the corrections of Table 5, leading to the final transformation equations between theoretical flux distribution and the Strömgren system:

$$b - y = (b - y)_0 + 0.883 ,$$
$$u - b = (u - b)_0 + 1.238 . \quad (2)$$

The colors with subscript 0 are the values computed from the models, e.g.,

$$(b - y)_0 = -2.5 \times \log \frac{\int_b S_b F_\lambda \, d\lambda}{\int_y S_y F_\lambda \, d\lambda} , \quad (3)$$

with the sensitivity functions S_b and S_y (Olson 1974). However,

TABLE 5

CORRECTIONS TO STRÖMGREN COLOR TRANSFORMATIONS FOR DB WHITE DWARFS

Scan − Observed	⟨Δ⟩	σ	N
$b - y$.....	0.058	0.034	16
$u - b$.....	−0.014	0.025	16

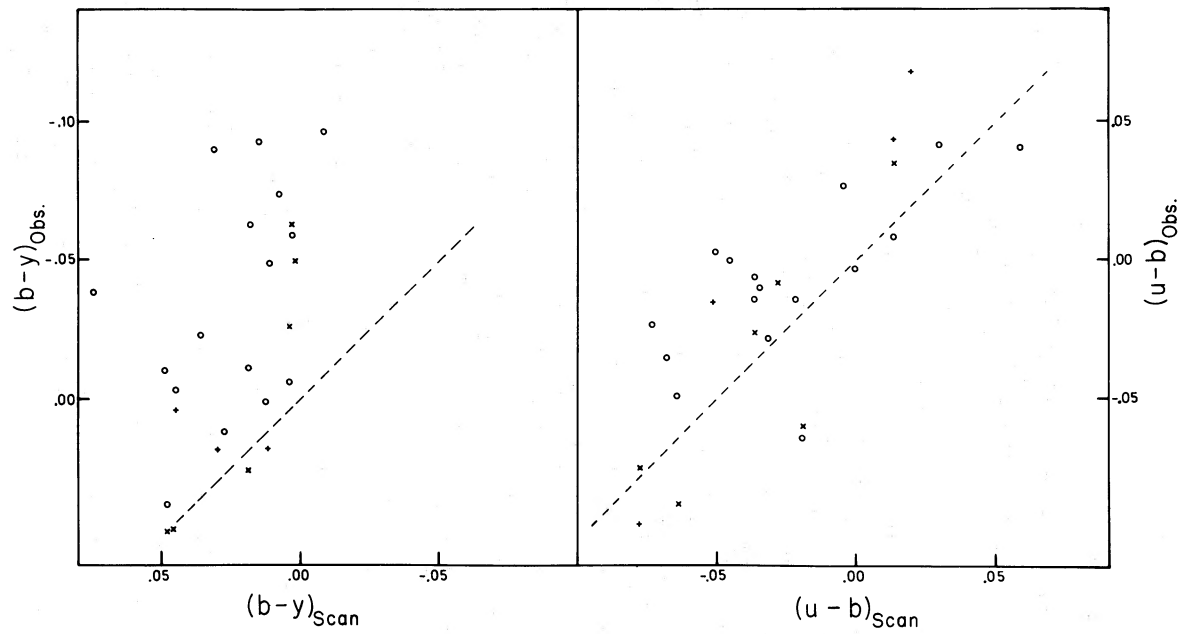

FIG. 5.—Calibration of Strömgren colors $b - y$ (*left*) and $u - b$ (*right*). Open circles from Wegner (1979, 1983), crosses from Graham (1972), and plus signs from Koester and Weidemann (1982).

the diagram (Fig. 5, *left*) for $b - y$ demonstrates that the range of observed values is about 3 times as large as that computed from the scans. The only explanation we can find is that the observational errors are obviously larger than assumed by the observers. Probably they are as large as the whole intrinsic spread for DB stars in the range 12,000–25,000 K, log g = 7.5–8.5, rendering the Strömgren colors of very limited value for a determination of atmospheric parameters, as already concluded by Koester, Schulz, and Wegner (1981).

VI. DISCUSSION AND SUMMARY

With the results of § IV, the average mass, the mass distribution, and the temperatures of the DB stars appear finally to be well determined. However, before we draw further conclusions, we have to assess the reliability of the results. First, concerning the dependence on absolute calibration: One of us (V. W.) has used the Schulz method (i.e., plotted the data in a R_{13}-R_{48} diagram) also for the Hayes-Latham (1975) calibration. The correction vectors depend on the standard stars used in an individual night and are given in Figure 6. The positions thus corrected are given in Figure 6. It appears that the expected cooling sequence with constant g is not fitted as well by the points in Figure 6 as by those in Figure 2. Thus, AB_{79} appears superior to the Hayes-Latham calibration. In this context we refer to the discussion by Greenstein (1982), who considered the possibility that the AB_{79} scale might be slightly too red. One of us (V. W.) also calculated the R_{13}-R_{48} distribution for older MCSP data on DB stars obtained at different occasions (J. L. Greenstein, private communication; Oke 1974): the scattering appears so large that no cooling sequence was discernible. We are thus forced to the conclusion that the clearer appearance of the DB cooling sequence is the result of three combined factors: homogeneous observing conditions and reduction procedures, evaluation method (Schulz indices, or least squares analysis), and a better calibration (AB_{79}).

Next, we have to consider the problem of the quality of the model atmospheres. During the progress of this work, the model atmospheres were changed from those of Koester (1980). The earlier analysis outlined in § III yielded results somewhat different from the later analysis. The grid points in the R_{13}-R_{48} diagram changed, for example, for log g = 8.0 from (R_{13}, R_{48}) = (−0.540, −1.117) to (−0.526, −1.108) for 12,000 K, and from (−0.755, −1.350) to (−0.704, −1.370) for 30,000 K. Thus, in the earlier analysis, the average g-value came out smaller, log $g \approx 7.5$, and the hotter stars, PG 175-39 and GD 358, were assigned improbably smaller-than-average values of log $g \approx 7.2$. It is thus apparent that minor changes in the calculated flux distribution, caused by a factor 15 reduction of metals (including C), suffice to influence the final results considerably. This being the case, one might of course revise the argument. How trustworthy are our derived values if the results depend so strongly on the models? Although a final statement cannot be made at this time, the total picture arising out of this investigation lends support to the conviction that model atmospheres for DB stars are finally converging. It has been a long process. Bues's (1970) first models were purely radiative, while Wickramasinghe (1972) included convection with He/H = 10^4 and metals/He = 10^{-2}. Shipman (1972) chose no hydrogen and solar abundances or no metals for his models but did not really consider the g-dependence. Wickramasinghe (1979) adopted He/H = 10^4 and metals/He = 1.5×10^{-4} (10^{-2} solar), whereas Koester (1980) selected models with He/H = 10^5 and metals/He = 1.5×10^{-5}. Needless to say, computing techniques and programs have also been

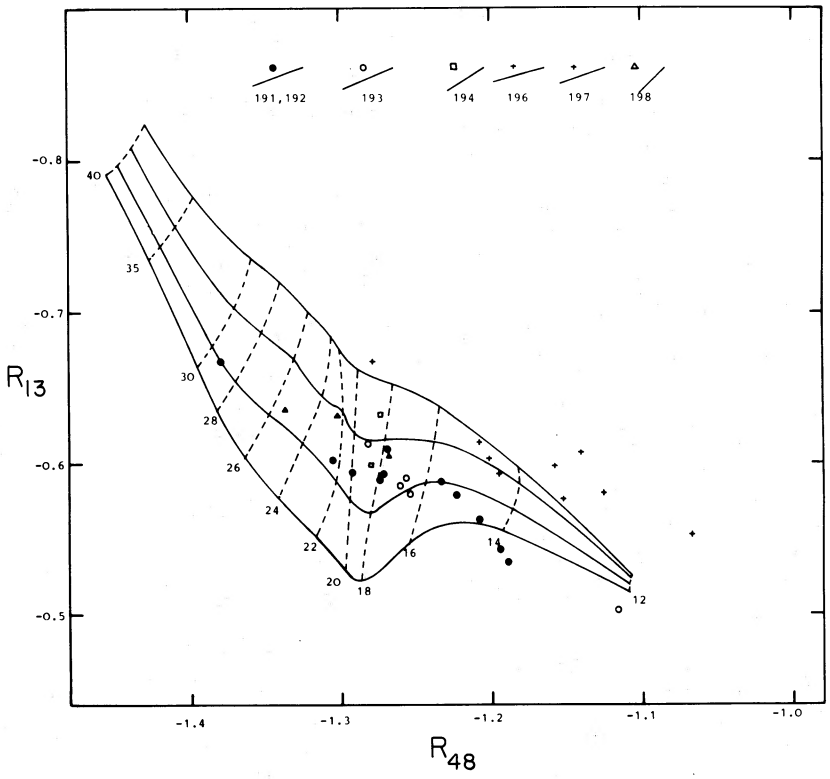

FIG. 6.—R_{13}-R_{48} diagram of DB stars, plotted on the Hayes-Latham (1975) calibration. Lines on top indicate the size of the shift from the AB_{79} to the Hayes-Latham position depending on the standards used on individual nights (cf. text and Fig. 2). The theoretical grid is identical to that in Fig. 2.

improved during the last decade. The surprisingly low upper limits put on C, O, and metal abundances for DC and C_2 stars, of which some are probably cooled-down DB stars, has finally determined the selection of the present set of abundances.

However, it must be cautioned that this convergence of model atmospheres is a first approximation in view of the fact that the cooler helium-rich atmospheres of DC and C_2 (and DF) stars exhibit a range of values, and thus we might also expect a *range* of C and metal abundances for the DB stars. This is evident in the case of GD 40 (Shipman and Greenstein 1983), which definitely has higher metal abundances than used here, as well as in the case of the strange "DB" G227-5 (cf. § II). If Koester's hypothesis of a carbon/helium transition layer reaching outward to the He convection zone is the correct explanation of C/He ratios of 10^{-6} or 10^{-7} at $T < 10{,}000$ K (Koester, Weidemann, and Zeidler–K. T. 1982), one should in general expect even smaller C abundances in the hotter DB range, in which convection does not reach deep enough to enrich the atmospheric layers with diffused carbon. This is in line with the observed fact that in the few DBs accessible to *IUE* (Wickramasinghe 1983; Koester, Vauclair, and Weidemann 1984) no C I or C II absorption lines are visible in the UV although theory predicts this even for C/He = 10^{-6}. Thus as far as C and metals are concerned, pure helium atmospheres are indeed a good approximation. However, the hydrogen content is not negligible, and H/He = 10^{-4}, 10^{-5}, or zero does make a difference for the DB stars. Again, the fact that some DBAs are known, e.g., G200-39 (Liebert *et al.* 1979) and probably the "DB" GD 323, originally included in our example, should serve as a warning against generalizations.

In summary, we feel that the model atmospheres used in this investigation are better than those which have been used in the past, and that therefore the results derived for the DB stars appear more reliable.

It has been demonstrated in § V that Strömgren photometry is not accurate enough to be of value for the $T_{\rm eff}/\log g$ determination in individual cases. The same holds, at present, unfortunately for information contained in the line spectra. Although one of us (J. B. O.) has obtained SIT spectra for all the objects in Table 1, and equivalent widths have been measured and calculated, e.g., for He I λ4471, comparison with model predictions showed so large a scatter that we did not include the data in this investigation. Comparison with synthetic spectra, still hampered partly by uncertainties in broadening theories, thus was left for future work, especially since an investigation evaluating line spectra has recently been published by Koester, Schulz, and Wegner (1981). Their study, however, is interesting from another point of view. Since it was based on the older set of Koester's models, it is not surprising that the mean mass they derived, 0.44 $M_\odot$, is smaller than that from this paper. However, the mass derived from the radius, which is calculated from the less model-sensitive temperature, in the six cases of DBs with known distances, came out larger, 0.54 $M_\odot$, and thus agrees much better with the result obtained in this paper.

It should be mentioned here that Shipman (1979) concluded that the mean radius for He-rich stars was not significantly different from that for the H-rich stars. Yet his sample included only three DB stars but many (24) cooler DC, C_2, DF, and DG degenerates, for which parallaxes or distances were known. For 17 DC and C_2 stars the new model atmospheres of Koester, Weidemann, and Zeidler–K. T. (1982) yielded $\langle M \rangle = 0.55$ $M_\odot$, compared with $\langle M \rangle = 0.58$ $M_\odot$ for the DAs (Koester, Schulz, and Weidemann 1979), thereby confirming Shipman's conclusion. But this cannot be taken as strong support for the DB result since, as discussed above (§ IV), the connection between DB and DC and C_2 stars is not yet safely established.

With the proviso mentioned above we finally add that Wickramasinghe and Reid (1983) arrive at $\langle M \rangle = 0.58$ $M_\odot$ by analysis of high-resolution line spectra for seven DB stars. For the three objects common to their survey and ours, LDS 749B, GD 40, and L930-80, their results compare with ours (in parentheses) as $T_{\rm eff} = 13{,}500 \pm 500$ ($13{,}150 \pm 190$), $\log g = 8.3 \pm 0.3$ (7.86 ± 0.4); $T_{\rm eff} = 14{,}250 \pm 750$ ($13{,}730 \pm 200$), $\log g = 8.2 \pm 0.3$ (7.85 ± 0.3); and $T_{\rm eff} = 15{,}550 \pm 500$ ($15{,}540 \pm 260$), $\log g = 8.3 \pm 0.3$ (8.14 ± 0.18).

As far as the temperatures are concerned, the scale appears now to be much better established. Since temperature is a decisive parameter for the occurrence of nonradial g-mode variability, and since GD 358, the first pulsating DB star discovered (Winget *et al.* 1982), is included in our ensemble, it is interesting that our result, $T_{\rm eff} = 25{,}000$ K, is comparatively high compared with theoretical estimates for the location of the instability strip ($\sim$19,000 K; Winget *et al.* 1982). *IUE* observations, on the other hand, predict a somewhat higher temperature ($\sim$28,000 K; Koester, Weidemann, and Vauclair 1983). The *IUE* UV flux calibration, however, especially for high temperatures, may not be accurate enough to allow a negative judgment on our scale.

For the cooler DBs our temperatures agree well with those derived from *IUE* fluxes by Wickramasinghe (1983). For LDS 749B he derived $T_{\rm eff} = 13{,}200 \pm 400$ K from the UV flux distribution, whereas our scale gives $13{,}150 \pm 190$ K from MCSP data. In this connection we must also mention a recent paper by Fontaine, Montmerle, and Michaud (1982) in which essentially negative results of X-ray observations of 10 DB stars with the *Einstein Observatory* are discussed. The temperatures listed in their Table 1 are in general above 30,000 K and appear systematically too high—first, since they were derived from $(G-R)$-$T_{\rm eff}$ relations based on older models and, second, since they used $(G-R)$ or even more doubtful transformations from $(B-V)$ and $(b-y)$ to $(G-R)$. Our newly derived temperatures are extremely different, in general about 10,000 K lower. In view of this fact the upper limits derived from the negative X-ray observations and conclusions about GD 205 as a potential X-ray source have to be completely revised.

In summary, the evidence has now become much stronger that DB and DA white dwarfs have similar masses and radii and that the differences in their atmospheric composition must be traced back to minor differences in the progenitor evolution. Especially the hypothesis that all DB stars are formed by merging of close binaries of the type of HZ 9 or GD 61-29, a possibility considered by Nather, Robinson, and Stover (1979) (see also Liebert 1980), must be ruled out. In comparing mean masses of DB and DA stars one should keep in mind, however, that a change in the absolute calibration from the Hayes-Latham to the AB_{79} program will also affect the DA results (Koester, Schulz, and Weidemann 1979) in the direction of somewhat higher average DA masses. Again, the masses derived from radii will probably be less affected, but this must and will be checked in a forthcoming investigation. What we can say now with some confidence is that the average mass of DB stars is $\langle M \rangle = 0.55 \pm 0.03$ $M_\odot$, and thus it falls into the typical range for final products of single-star evolution toward the white dwarf stage (Weidemann and Koester 1983). If DB characteristics are produced by a late thermal pulse of a He-

shell in nuclei of planetary nebulae (like Abell 30 and Abell 78; see Iben *et al.* 1983) or by (neglected) parameters like rotation and/or magnetic fields (Weidemann 1975), which influence the mass loss history, the final outcome even for equal progenitor masses remains uncertain.

Part of this work was carried out when one of us (V. W.) was a Guest Investigator at the California Institute of Technology, whose hospitality is gratefully acknowledged. We also want to thank Professor Jesse L. Greenstein for kindly providing earlier MCSP data. This work was supported in part by the National Aeronautics and Space Administration through grant NGL 05-002-134 to J. B. Oke.

REFERENCES

Bues, I. 1970, *Astr. Ap.*, **7**, 91.
Fontaine, G., Montmerle, T., and Michaud, G. 1982, *Ap. J.*, **257**, 695.
Graham, J. A. 1972, *A.J.*, **77**, 144.
Greenstein, J. L. 1969, *Ap. J.*, **158**, 281.
———. 1976, *Ap. J.*, **210**, 524.
———. 1982, *Ap. J.*, **258**, 661.
———. 1984, *Ap. J.*, **276**, 602.
Griem, H. R. 1974, *Spectral Line Broadening by Plasmas* (New York: Academic Press).
Hamada, T., and Salpeter, E. E. 1961, *Ap. J.*, **134**, 683.
Hayes, D. S., and Latham, D. W. 1975, *Ap. J.*, **197**, 593.
Iben, I., Jr., Kaler, J. B., Truran, J. W., and Renzini, A. 1983, *Ap. J.*, **264**, 605.
Koester, D. 1972, *Astr. Ap.*, **16**, 459.
Koester, D. 1976, *Astr. Ap.*, **52**, 415.
———. 1979, in *IAU Colloquium 53, White Dwarfs and Variable Degenerate Stars*, ed. H. Van Horn and V. Weidemann (Rochester: University of Rochester), p. 130.
———. 1980, *Astr. Ap. Suppl.*, **39**, 401.
Koester, D., Schulz, H., and Wegner, G. 1981, *Astr. Ap.*, **102**, 331.
Koester, D., Schulz, H., and Weidemann, V. 1979, *Astr. Ap.*, **76**, 262.
Koester, D., Vauclair, G., and Weidemann, V. 1984, in preparation.
Koester, D., and Weidemann, V. 1982, *Astr. Ap.*, **108**, 406.
Koester, D., Weidemann, V., and Vauclair, G. 1983, *Astr. Ap.*, submitted.
Koester, D., Weidemann, V., and Zeidler-K. T., E.-M. 1982, *Astr. Ap.*, **116**, 147.
Liebert, J. 1980, *Ann. Rev. Astr. Ap.*, **18**, 363.
Liebert, J., Gresham, M., Hege, E. K., and Strittmatter, P. A. 1979, *A.J.*, **84**, 1612.
Liebert, J., and Wesemael, F. 1983, preprint.
McCook, G. P., and Sion, E. M. 1977, *Villanova Univ. Obs. Contr.*, No. 2.
Nather, R. E., Robinson, E. L., and Stover, R. J. 1979, in *IAU Colloquium 53, White Dwarfs and Variable Degenerate Stars*, ed. H. Van Horn and V. Weidemann (Rochester: University of Rochester), p. 453.
Oke, J. B. 1974, *Ap. J. Suppl.*, **27**, 21.
Oke, J. B., and Gunn, J. E. 1983, *Ap. J.*, **266**, 713.
Olson, E. C. 1974, *Pub. A.S.P.*, **86**, 80.
Schulz, H. 1977, thesis, University of Kiel.
———. 1978, *Astr. Ap.*, **68**, 75.
Shipman, H. L. 1972, *Ap. J.*, **177**, 723.
———. 1979, *Ap. J.*, **228**, 240.
Shipman, H. L., and Greenstein, J. L. 1983, *Ap. J.*, **266**, 761.
Sion, E. M. 1979, in *IAU Colloquium 53, White Dwarfs and Variable Degenerate Stars*, ed. H. Van Horn and V. Weidemann (Rochester: University of Rochester), p. 245.
Sion, E. M., and Liebert, J. 1977, *Ap. J.*, **213**, 468.
Vauclair, G., and Reisse, C. 1977, *Astr. Ap.*, **61**, 415.
Wegner, G. 1979, *A.J.*, **84**, 1384.
———. 1983, *Ap. J.*, **268**, 282.
Weidemann, V. 1967, *Zs. Ap.*, **67**, 286.
———. 1975, in *Problems in Stellar Atmospheres and Envelopes*, ed. B. Baschek, W. H. Kegel, and G. Traving (Berlin: Springer-Verlag), p. 173.
———. 1977, *Astr. Ap.*, **61**, L27.
———. 1979, in *IAU Colloquium 53, White Dwarfs and Variable Degenerate Stars*, ed. H. Van Horn and V. Weidemann (Rochester: University of Rochester), p. 206.
Weidemann, V., and Koester, D. 1983, *Astr. Ap.*, in press.
Wickramasinghe, D. T. 1972, *Mem. Roy. Astr. Soc.*, **76**, 129.
———. 1979, in *IAU Colloquium 53, White Dwarfs and Variable Degenerate Stars*, ed. H. Van Horn and V. Weidemann (Rochester: University of Rochester), p. 35.
———. 1983, *M.N.R.A.S.*, **203**, 903.
Wickramasinghe, D. T., and Reid, N. 1983, *M.N.R.A.S.*, **203**, 887.
Winget, D. E., Robinson, E. L., Nather, E. R., and Fontaine, G. 1982, *Ap. J. (Letters)*, **262**, L11.

D. KOESTER and V. WEIDEMANN: Institut für Theoretische Physik und Sternwarte, University of Kiel, Leibnizstrasse, 2300 Kiel, F. R. Germany

J. B. OKE: Department of Astronomy 105-24, California Institute of Technology, Pasadena, CA 91125